Correlation Analysis Between Urban Green Space Morphological Indicators and Cooling Efficiency

Yihan Chang *

School of Geography and Tourism, Shaanxi Normal University, Xi'an, China

* Corresponding Author Email: changyihan05@snnu.edu.cn

Abstract. In recent years, urban green spaces have been extensively investigated for their significant contribution to mitigating the urban heat island effect. Yet, while cooling intensity has been the dominant focus of most previous research, cooling efficiency and cooling distance remain comparatively underexplored. Based on Landsat 8 remote sensing data, an urban green space morphology-based efficiency diagnosis system was established for the built-up area of Xi'an. A total of 146 green space patches were identified, and their morphological attributes, including area, shape index, circularity, compactness, and elongation, were quantified. Patch information and land surface temperature data were jointly used to estimate cooling intensity, cooling distance, and cooling efficiency. A notably strong positive correlation emerged between cooling intensity and cooling efficiency ($r = 0.84$), implying that green spaces exhibiting stronger cooling performance also tend to operate more efficiently on a per-area basis. Cooling intensity was positively related to cooling distance ($r = 0.33$), suggesting that patches with stronger cooling effects tended to influence a larger surrounding area. In contrast, green space area showed weak correlations with cooling intensity, cooling distance, and cooling efficiency ($r = -0.06$, -0.10, and -0.08, respectively). The results suggest that simply increasing green space area may not lead to better cooling performance. These results provide a useful reference for green space planning in high-density cities. Where land resources are limited, improving the internal structure and connectivity of green spaces may be more effective than simply increasing patch size or creating regular-shaped green spaces.

Keywords: Urban green space; spatial morphology; thermal regulation; Landsat 8 imagery; Xi'an, China.

1. Introduction

Thermal stress in urban settings has been exacerbated by the growing frequency of extreme heat events [1]. Meanwhile, the expansion of urban areas has greatly enlarged the extent of impervious cover, which in turn worsens the urban heat island effect and compromises both environmental quality and human thermal comfort [2]. As an important nature-based solution, urban green spaces mitigate surface warming through shading and evapotranspiration processes [3]. Previous studies have reported that different forms of green infrastructure can lower ambient temperature by approximately 1.1-4.6°C [4]. Therefore, increasing urban greening has become one of the main approaches for mitigating urban heat for mitigating urban heat in planning practice [5].

Existing research mostly focuses on the single indicator of cooling intensity of urban green spaces, with relatively insufficient attention paid to cooling area, cooling efficiency, and their comprehensive evaluation [6-9]. Previous studies have shown that factors such as green space area, spatial configuration, and morphological characteristics can influence urban cooling effects, which has contributed to a better understanding of the cooling mechanisms of urban green spaces [7-9]. However, most existing studies mainly focus on the evaluation of cooling effects, while the quantitative description of green space morphology and the assessment of cooling efficiency still lack a relatively integrated technical approach. This limitation restricts the application of green space cooling research in detailed urban planning and optimization practices [10].

Accordingly, the present study aims to explore the linkage between the morphological characteristics of urban green spaces and their cooling efficiency. Based on green space patch extraction, morphological parameter calculation, comprehensive evaluation, and visualization analysis, this study analyzes several morphological characteristics, including area, shape index,

circularity, compactness and elongation. A corresponding evaluation framework is established to explore how different morphological features affect cooling efficiency and to provide a reference for the optimization of urban green space planning.

2. Data and Methods

2.1. Data Source and Preprocessing

2.1.1. Data source

The remote sensing data used in this study were sourced from the Geospatial Data Cloud Platform (www.gscloud.cn), with Landsat 8 Operational Land Imager (OLI) and Thermal Infrared Sensor (TIRS) satellite imagery selected [11]. The Landsat 8 satellite has a revisiting period of 16 days, with spatial resolutions including 30m for multispectral bands, 15m for panchromatic bands, and 100m for thermal infrared bands (all resampled to 30m for this study). The imagery was acquired during the summer months (June to September) during clear and cloudless conditions (cloud cover <10%) to ensure the accuracy of land surface temperature inversion. Specific image parameters are shown in Table 1.

Table 1. The Landsat 8 image band information used in the study.

Band Name	Band Number	Wavelength range (μm)	Spatial resolution (m)	purpose
Red band	Band 4	0.64—0.67	30	Vegetation index calculation
Near-infrared band	Band 5	0.85—0.88	30	Vegetation index calculation
Thermal Infrared Band	Band 10	10.60—11.19	30	Land surface temperature retrieval

2.1.2. Data preprocessing

Before analysis, the Landsat 8 Level-2 imagery was preprocessed to improve data reliability and minimize the influence of sensor characteristics and atmospheric effects. The Level-2 products provided by the USGS had already undergone radiometric calibration and atmospheric correction before being downloaded. Surface reflectance (SR) was derived from the original DN values using the scale factor specified in the Landsat 8 Level-2 metadata [12]:

$$\rho = DN \times 0.0000275 - 0.2 \quad (1)$$

Where ρ represents surface reflectance, with values ranging from 0 to 1. The resulting reflectance values were subsequently used for NDVI calculation, green space extraction, and vegetation-related analysis. Pixels with DN values ≤0 were removed before further processing to reduce the influence of invalid data.

Using the scale factor contained in the Level-2 product metadata, it derived brightness temperature from the thermal band and subsequently obtained land surface temperature (LST) from the same thermal infrared data [12]:

$$T_K = DN \times 0.00341802 + 149.0 \quad (2)$$

Where TK represents temperature in Kelvin. The Kelvin temperature was further converted into Celsius temperature using:

$$TLST = TK - 237.15 \quad (3)$$

The derived LST data were used to describe the spatial distribution of surface thermal conditions and to calculate the cooling characteristics of urban green spaces. During processing, pixels with DN values ≤ 0 were regarded as invalid and assigned a default temperature of 25°C to keep the temperature raster continuous.

2.2. Green Patch Extraction Method

Green space patch extraction provides the basis for the following morphological analysis. Green space patches were extracted from Landsat 8 images according to the information contained in the red and near-infrared bands. The whole extraction process consisted of four main steps: NDVI calculation, threshold-based segmentation, morphological processing, and connected component analysis.

2.2.1. NDVI calculation

To characterize vegetation distribution across the study area, it adopted the Normalized Difference Vegetation Index (NDVI), which is derived from the reflectance contrast between the red and near-infrared bands—healthy vegetation tends to exhibit low reflectance in the red band while showing high reflectance in the near-infrared band [13]. NDVI calculation relied on surface reflectance data from Landsat 8 Level-2 products, specifically bands 4 (red) and 5 (near-infrared), computed on a per-pixel basis. The resultant NDVI values fell between −1 and 1, with larger values pointing to denser vegetation.

2.2.2. Threshold segmentation

The NDVI image was then converted into a binary mask for separating vegetated and non-vegetated areas. An empirical threshold of 0.40 was selected to separate vegetation from non-vegetation. Pixels with NDVI values exceeding the threshold were marked as green land of 1 (green land), whereas all other pixels were assigned a value of 0 (non-green land) [14].

The selected threshold directly affects the accuracy of green space extraction. A relatively high threshold may omit sparsely vegetated areas, whereas a lower threshold may include non-vegetated surfaces with similar spectral characteristics.

2.2.3. Morphological processing

The initial binary mask may contain isolated pixels and small gaps that reduce the reliability of subsequent morphological analysis. Morphological opening and closing operations were carried out on the binary mask to refine the extracted patches [15].

Isolated pixels were eliminated through an opening procedure (erosion prior to dilation), whereas closing (dilation followed by erosion) served to seal minor gaps inside the identified patches. A square structuring element of 3×3 was adopted for both operations, and the iteration count was tuned based on the performance of the extraction process.

Compared with the original pixel-based implementation, the optimized image-processing functions provided by the scientific computing library made the processing much faster.

2.2.4. Extracting the largest connected component

After morphological processing, multiple disconnected green space patches remained in the binary mask. Connected component analysis was used to identify individual green space patches for subsequent morphological analysis. The BFS algorithm was used to label connected regions satisfying the predefined area threshold, and each retained patch was treated as an individual unit for subsequent analysis [16].

A minimum patch size of 50 pixels was adopted to eliminate small regions caused by classification noise or scattered vegetation. Patches below this threshold were removed to improve the robustness of the extracted green space dataset.

3. Results and Analysis

3.1. Green Patch Extraction and Morphological Features

The Landsat 8 OLI image cropped based on the boundary of Xi'an built-up area was imported into the system [17]. By employing the NDVI threshold segmentation method (θ=0.40) combined with morphological opening and closing operations, a total of 146 independent green space patches were

extracted, covering an area of approximately 13,573.44 ha, which accounts for 35.0% of the total built-up area.

From the perspective of spatial distribution, large patches (such as the Tang Dynasty Furong Garden) are mainly concentrated in urban parks and university campuses, while a large number of small patches are scattered throughout the built-up area. The distribution of patch areas is extremely uneven: the largest patch covers an area of 1906.56 ha, the smallest patch covers an area of 18.00 ha, and the average patch area is 92.97 ha. The largest patch area is 20.5 times the average patch area and 106 times the smallest patch area.

The statistical results of morphological indicators are presented in Table 2. The average shape index is 2.80, the average circularity is 0.175, the average compactness is 0.67, and the average elongation is 2.30.

Table 2. Overall morphological characteristics of green patch.

Indicator	numerical value	unit
Total green space area	13573.44	ha
Number of green patches	146	piece
Average patch area	92.97	ha
Maximum patch area	1906.56	ha
Minimum patch area	18	ha
Average shape index	2.80	—
Average circularity	0.175	—
Average compactness	0.67	—
Average extensibility	2.30	—

Note: The area statistics are all obtained based on the green patch extraction method described in Section 2.2.

3.2. Correlation between morphological indicators and cooling efficiency

To explore the relationship between various morphological indicators and cooling efficiency, the corresponding algorithm was used to calculate the Pearson correlation coefficient. The results are shown on Fig. 1.

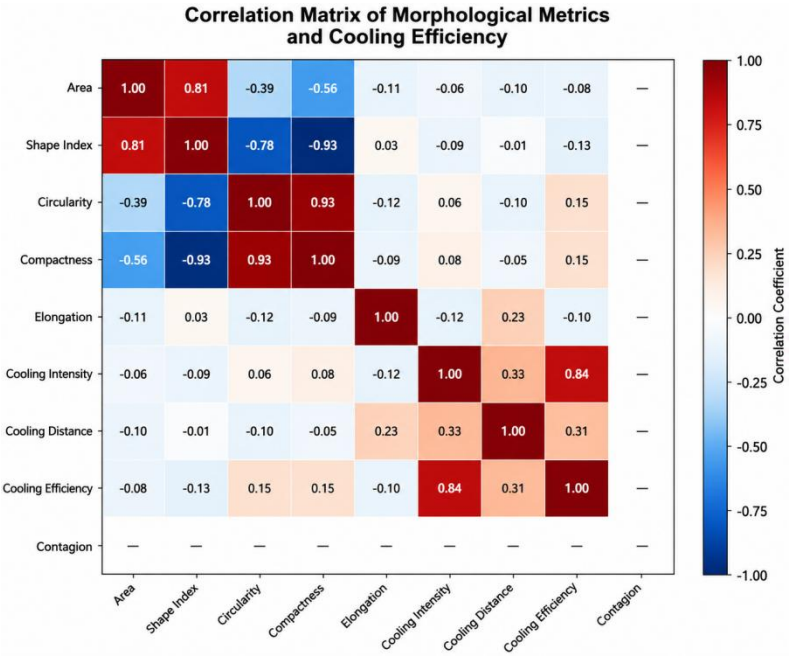


Fig 1. Correlation matrix between morphological indicators and cooling efficiency.

Note: All green space patches extracted in this study are single connected components with a contagion index of 100% and thus were not included in the correlation analysis.

Based on the correlation matrix, the cooling intensity and cooling efficiency exhibit the highest degree of synergy (r=0.84), and there is also a moderate positive correlation with cooling distance (r=0.33). According to the statistics of different efficiency levels, a total of 146 green space patches were identified, including 2 high-efficiency green spaces (≥80 points), accounting for 1.37%, and 144 medium-efficiency green spaces (50–79 points), accounting for 98.63%. The green space patches identified in this study all belong to medium or above efficiency levels, with no low-efficiency green spaces (<50 points) identified. The average cooling intensity of high-efficiency green spaces is 0.75 ℃, the average cooling distance is 280.0 m, and the average cooling efficiency is 2.76. Meanwhile, the corresponding values for medium-efficiency green spaces are 0.13 ℃, 247.6 m, and 0.24, respectively.

The relationships between green area and cooling-related indicators were relatively weak. The correlation coefficients between green area and cooling intensity, cooling distance, and cooling efficiency were -0.06, -0.10, and -0.08, respectively. Most morphological indicators also showed weak correlations with cooling performance, with correlation coefficients below 0.20 in absolute value. Among these indicators, elongation showed a weak positive correlation with cooling distance (r = 0.23), while the other morphological variables showed limited relationships with cooling intensity, cooling distance, and cooling efficiency.

Strong correlations were also observed among some morphological indicators. Area showed a positive correlation with shape index (r = 0.81), while shape index was negatively correlated with compactness (r = -0.93). Circularity and compactness exhibited a strong positive correlation (r = 0.93). These relationships suggest that several morphological indicators may reflect similar aspects of green space configuration.

4. Discussion

4.1. Main Findings and Mechanism Explanation

The analysis showed a strong positive correlation between cooling intensity and cooling efficiency (r = 0.84), whereas cooling intensity showed a moderate correlation with cooling distance (r = 0.33). These results indicate that green spaces with stronger cooling performance usually have higher cooling efficiency and a larger cooling range in high-density urban areas.

However, the relationships between green space morphology and cooling performance were much weaker than expected. Green space area showed only weak correlations with cooling intensity, cooling distance, and cooling efficiency ($|r| < 0.10$), while the relationships between shape-related metrics and cooling indicators also remained weak (generally $|r| < 0.16$). This differs from the conclusion reported by Li et al., who identified green space area and shape compactness as major factors influencing cooling performance [10]. One reason may be that, in high-density cities, the influence of green space morphology may be weakened by surrounding buildings and anthropogenic heat sources. Therefore, cooling performance may depend more on local microclimatic conditions than on green space morphology itself.

The relationship between elongation and cooling distance was weak but positive (r = 0.23), suggesting that elongated green spaces tend to influence a slightly larger surrounding area than more compact patches. This may be because many elongated green spaces in Xi'an are located along major roads, allowing cooler air to spread farther through these green corridors.

4.2. Research Limitations and Prospects

There are still several limitations in this study. First, independent green space patches were used as analytical units. Each extracted patch was a single connected component. Therefore, the contagion index showed no variation and was not included in the correlation analysis. A further drawback concerns the 30 m spatial resolution inherent to Landsat imagery, which could lead to an underestimation of the actual green space coverage within the built-up area [18]. The cooling assessment model was also relatively simple and did not include factors such as wind conditions,

building obstruction, surrounding building density, or road distribution. This may partly explain why the correlations between morphology and cooling performance were generally weak [19]. In future work, higher-resolution remote sensing images, landscape connectivity indicators, and more environmental variables can be included to improve the evaluation of urban green space cooling performance.

5. Conclusion

This study takes the built-up area of Xi'an as the research object and based on Landsat 8 remote sensing images and an independently developed urban green space morphological efficiency diagnosis system, conducts a correlation analysis between the morphological characteristics and cooling efficiency of 146 green space patches. The research results show that there is a high positive correlation between cooling intensity and cooling efficiency (r=0.84), and a moderate positive correlation with cooling distance (r=0.33), indicating that green spaces with better cooling effects usually have higher cooling efficiency per unit area and can affect a larger surrounding area.

According to the correlation analysis, green space area exhibited only weak relationships with cooling intensity (r = -0.06), cooling distance (r = -0.10), and cooling efficiency (r = -0.08). Traditional morphological indicators such as shape index, circularity, and compactness also show no significant linear relationship with the cooling indicators, indicating that a single morphological indicator has limited explanatory power for the cooling effect of green spaces. Among the examined morphological indicators, elongation had a weak positive relationship with cooling distance (r = 0.23). This finding indicates that elongated green spaces may influence a relatively wider area than other spatial forms.

The results also show that green space size alone does not necessarily guarantee better cooling performance in high-density urban areas. When land resources are limited, optimizing green space configuration and spatial structure may provide more benefits than simply enlarging patch areas or creating regular shapes.

References

[1] Bai X Y, Yu Z W, Wang B Y, et al. Quantifying threshold and scale response of urban air and surface temperature to surrounding landscapes under extreme heat. Building and Environment, 2024, 247: 111029.

[2] Yu Z W, Yang G Y, Lin T, et al. Exposure ecology drives a unified understanding of the nexus of (urban) natural ecosystem, ecological exposure, and health. Ecosystem Health and Sustainability, 2024, 10: 0165.

[3] Hami A, Abdi B, Zarehaghi D, et al. Assessing the thermal comfort effects of green spaces: A systematic review of methods, parameters, and plants' attributes. Sustainable Cities and Society, 2019, 49: 101634.

[4] Chen W Q, Pan J H, Quan S J, et al. Scalable impact of urban green infrastructure on urban climate: A critical review. Renewable and Sustainable Energy Reviews, 2026, 226: 116259.

[5] Bowler D E, Buyung-Ali L, Knight T M, et al. Urban greening to cool towns and cities: A systematic review of the empirical evidence. Landscape and Urban Planning, 2010, 97(3): 147-155.

[6] Galalizadeh S, Morrison-Saunders A, Horwitz P, et al. The cooling impact of urban greening: A systematic review of methodologies and data sources. Urban Forestry & Urban Greening, 2024, 95: 128157.

[7] Li F, Wu C, Chen H, et al. Optimizing urban green space ecosystem services for climate resilience: A multi-dimensional assessment of urban park cooling effects. Forests, 2026, 17(3): 383.

[8] Han M, Zhang T, Si Z. Optimizing urban blue-green space in climate adaptive planning: A systematic review of threshold value of efficiency thresholds. Landscape Ecology, 2025, 40: 13.

[9] Jiang X F, Ma T, Liang J P, et al. The greener the cooler? Nonlinear thresholds in the cooling effects of urban blue-green spaces and implications for sustainable planning in the Yangtze River Delta. Urban Climate, 2025, 64: 102679.

[10] Li Y L, Ren C, Ho J Y E, et al. Landscape metrics in assessing how the configuration of urban green spaces affects their cooling effect: A systematic review of empirical studies. Landscape and Urban Planning, 2023, 239: 104842.

[11] Geospatial Data Cloud. Landsat 8 OLI/TIRS satellite image products. Computer Network Information Center, Chinese Academy of Sciences, 2024. https://www.gscloud.cn.

[12] USGS. How do I use a scale factor with Landsat Level-2 science products? U.S. Geological Survey.

[13] Tucker C J. Red and photographic infrared linear combinations for monitoring vegetation. Remote Sensing of Environment, 1979, 8(2): 127-150.

[14] Wang H, Li X B, Ying G, et al. The methods of simulating vegetation growing season are based on NOAA NDVI. Progress in Geography, 2006, 25(6): 21-32.

[15] Haralick R M, Sternberg S R, Zhuang X. Image analysis using mathematical morphology. IEEE Transactions on Pattern Analysis and Machine Intelligence, 1987, 9(4): 532-550.

[16] Zhou L L, Ye Y T, Liu L, et al. BFS-based multi-core parallel connected component detection algorithm. Opto-Electronic Engineering, 2011, 38(7).

[17] Zhang S J, Li M, Dan B Y, et al. Urban built environment evaluation unit dataset based on multi-source data (2022). Journal of Global Change Data & Discovery, 2025.

[18] Yang J, Li Z, Zhou Y Y, et al. Systematic overestimation of urban parks' cooling effects may mislead heat-governance-oriented park planning. Landscape and Urban Planning, 2025, 264: 105467.

[19] Lyu R F, Zhou L, Guo Z C, et al. Optimization of urban cooling network informed by actual flow of cooling service provided by urban green space from a 3D perspective. Urban Forestry & Urban Greening, 2025, 113: 129109.